Supporting Information for

Increasing Oxygen Vacancy of CeO_2 Nanocrystals by Ni Doping and reduced Graphene Oxides Decoration towards the Electrocatalytic Hydrogen Evolution

Yang Xu[a,b,‡], Xiaodong Hao[a,‡,], Xishuo Zhang[a,b], Zhuangzhuang Hu[b], Yujiao Chen[b], Xinyi Feng[a,b], Danting Li[b], Wen Liu[c], Fangyuan Hao[c], Xingang Kong[b], Chaozheng He[d], Shufang Ma[a], Bingshe Xu[a]*

[a]Materials Institute of Atomic and Molecular Science, Shaanxi University of Science & Technology, Xi'An 710021, China

[b]School of Materials Science and Engineering, Shaanxi University of Science & Technology, Xi'an 710021, China

[c]School of Mathematics and Statistics, Shaanxi Normal University, Xi'an 710119, China

[d] Institute of Environmental and Energy Catalysis, Shaanxi Key Laboratory of Optoelectronic Functional Materials and Devices, School of Materials Science and Chemical Engineering, Xi'an Technological University, Xi'an 710021, People's Republic of China

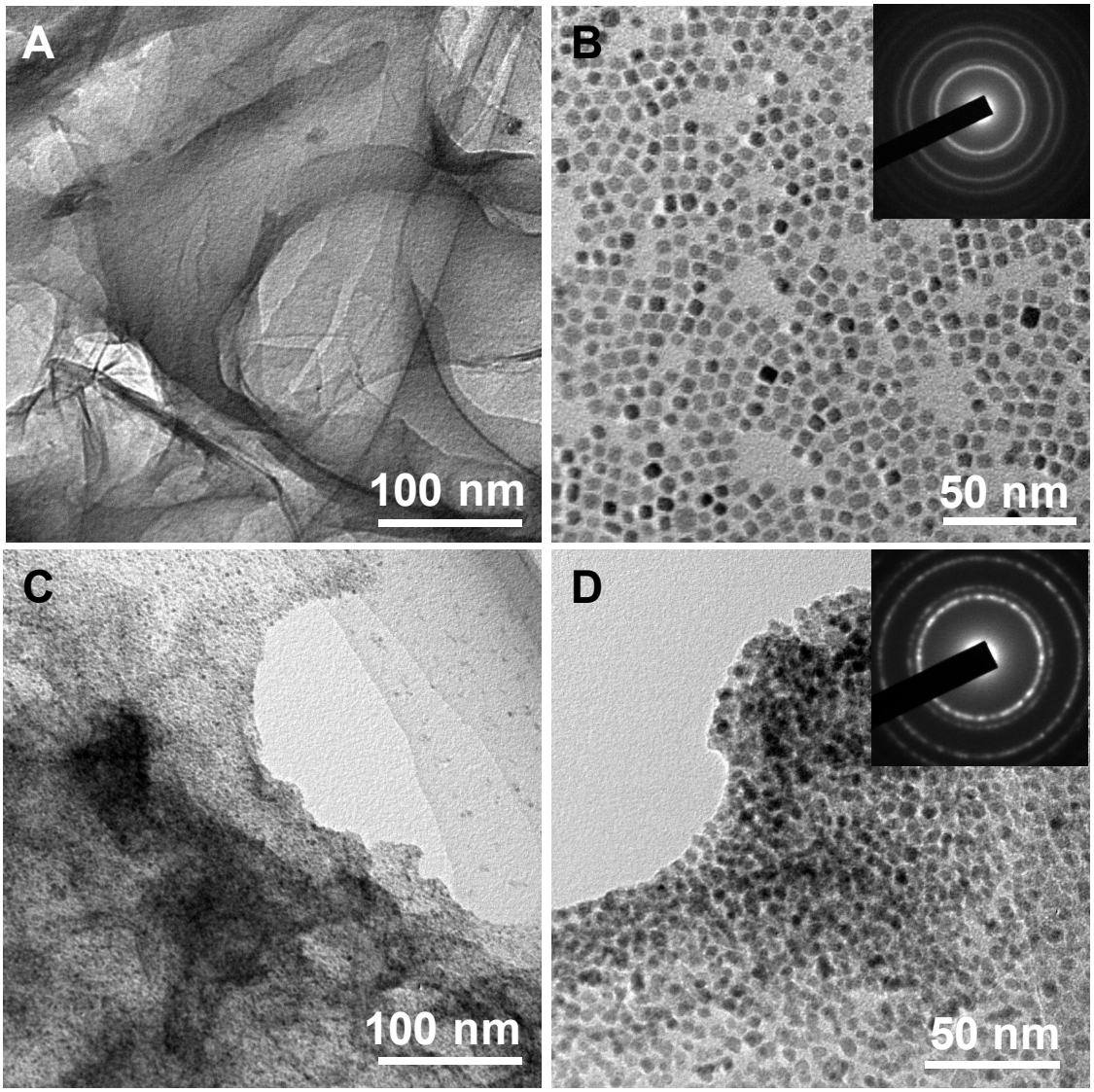

Figure S1. TEM images of the pristine rGO in (A), the as-synthesize CeO_2 NCs in (B) and the CeO_2/rGO NCPs in (C, D).

As can be seen, the pristine rGO is composed of layered thin platelets in a large scale in Figure S1A, and after the imcorporation of the uniform CeO_2 NCs (Figure S1B), the almost uniform distribution of CeO_2 NCs upon rGO sheets is obtained (Figure S1C, D).

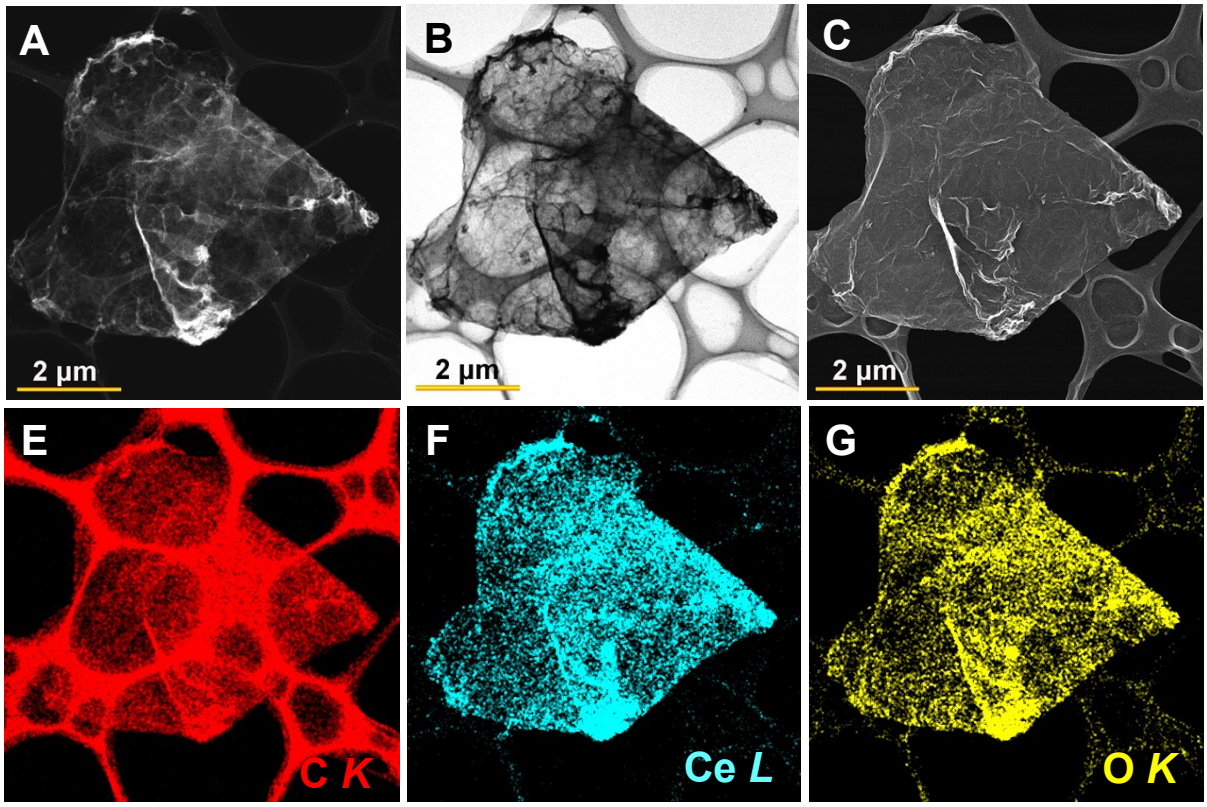

Figure S2 The STEM images of CeO_2/rGO NCPs and elemental analysis: (A) HADDF-STEM, B) ABF-STEM, C) SEI-STEM, E-G) separate elemental maps of carbon *K* edge (red), cerium *L* edge (cyan), and oxygen *K* edge (yellow), respectively.

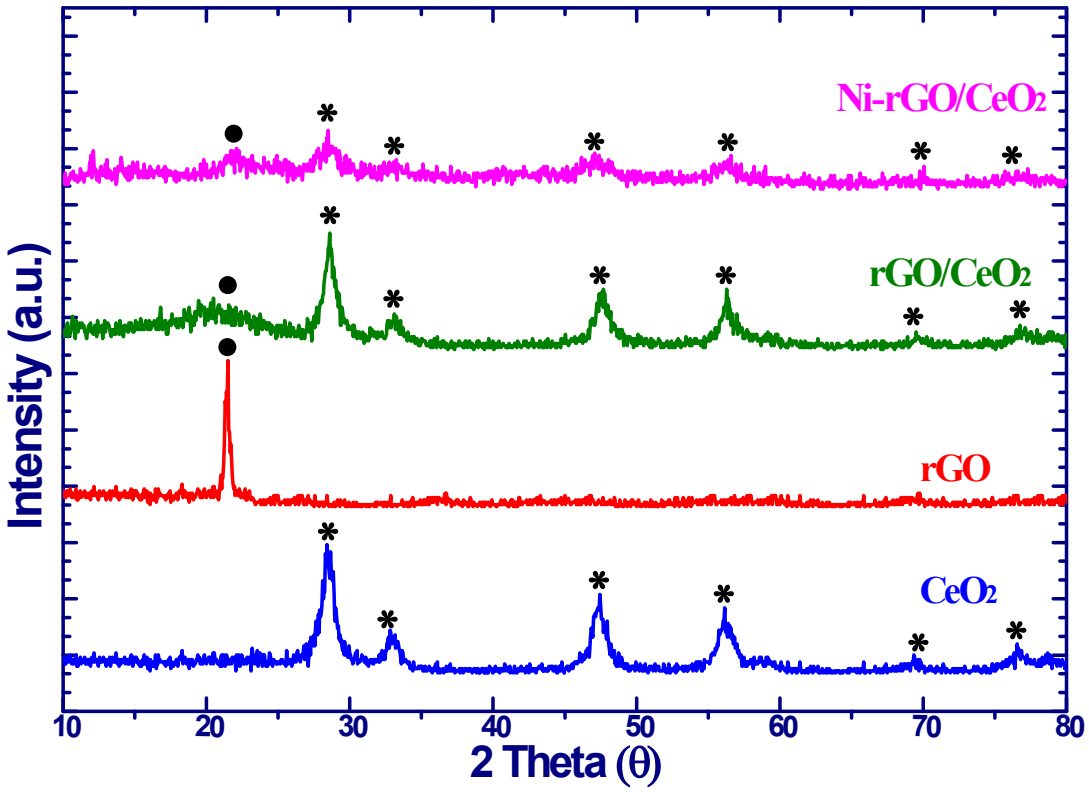

Figure S3. XRD spectra of as-synthesize CeO_2 NCs, the pristine rGO, the CeO_2/rGO NCPs, and Ni-CeO_2/rGO NCPs.

The XRD spectrum of the as-synthesized CeO_2 NCs shows the good crystallinity of with four major peaks located around 28.4º, 32.8º, 47.5º, 56.2º, which can be assigned to the 111, 200, 220 and 311 diffraction of the fluorite-cubic structure of CeO_2 (JCPDS, 34-0394).[1] Subsequently, the peak strength and peak width of rGO around 22.1º is degenerated in the large extent, comparing to that of the pristine rGO, while the the good crystallinity of the CeO_2 NCs is retained.

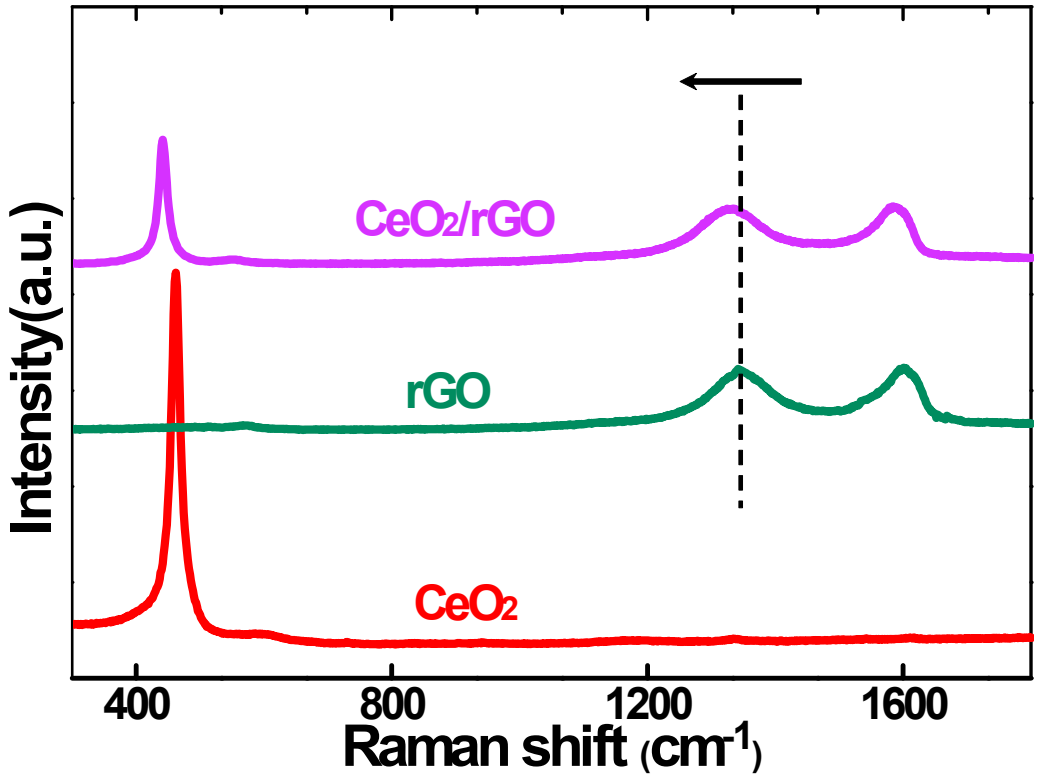

Figure S4 Raman spectra of the pristine rGO, CeO_2 NCs, and rGO/CeO_2 NCPs, respectively.

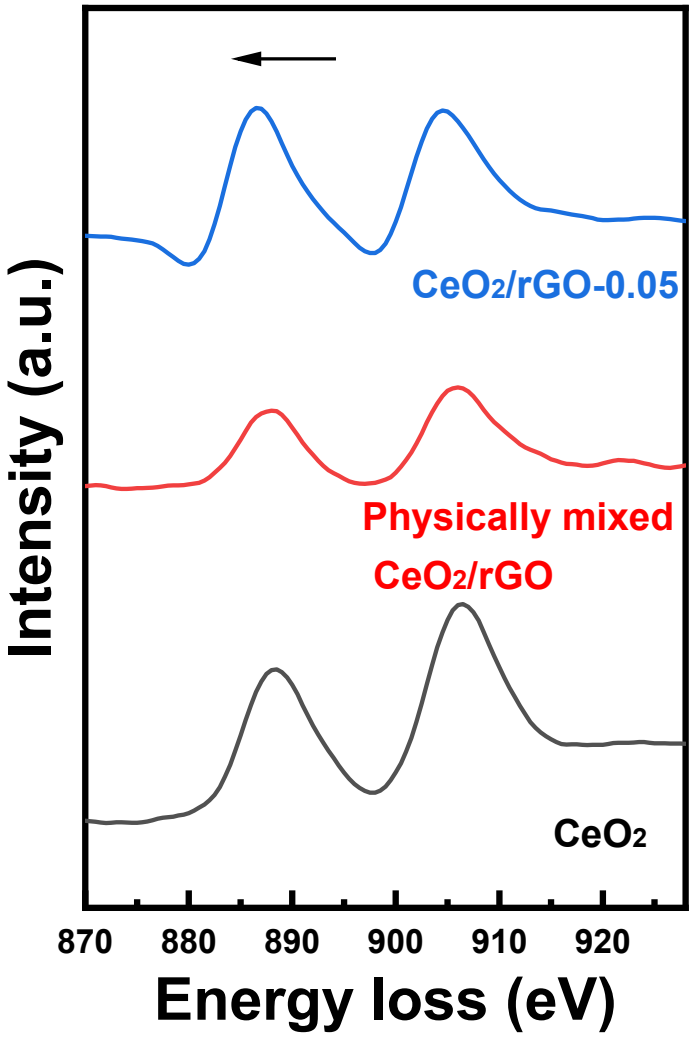

Figure S5. EELS spectra of the *M* edge of Ce for pristine CeO_2, physically mixed CeO_2/rGO and CeO_2/rGO-0.05.

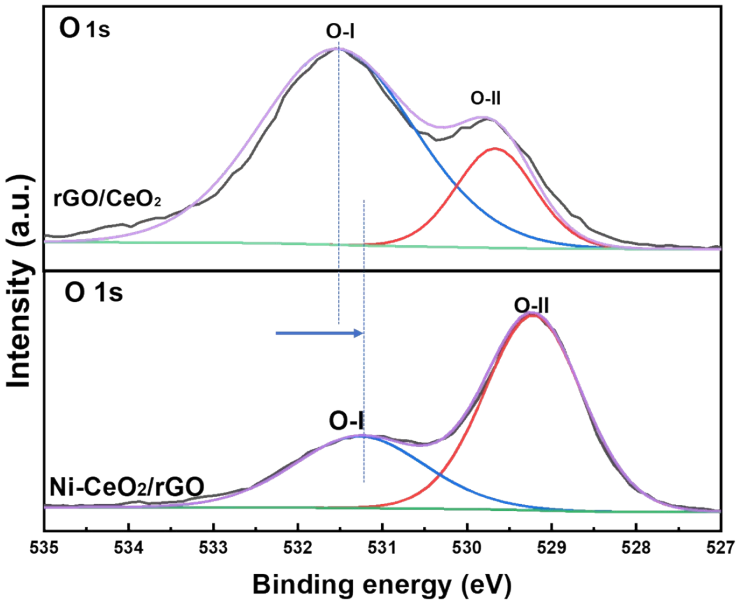

Figure S6. The split spectrum of O *1s* of the CeO_2/rGO and Ni-CeO_2/rGO NCPs

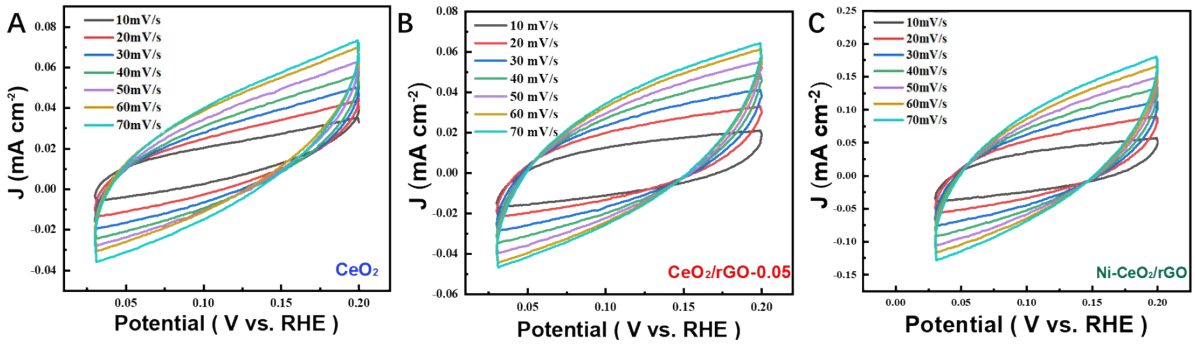

Figure S7. Typical cyclic voltammetry curves of (A) the pristine CeO_2, (B) CeO_2/rGO-0.05, and (C) Ni-CeO_2/rGO-0.05 NCPs in 1M KOH with different scan rates.

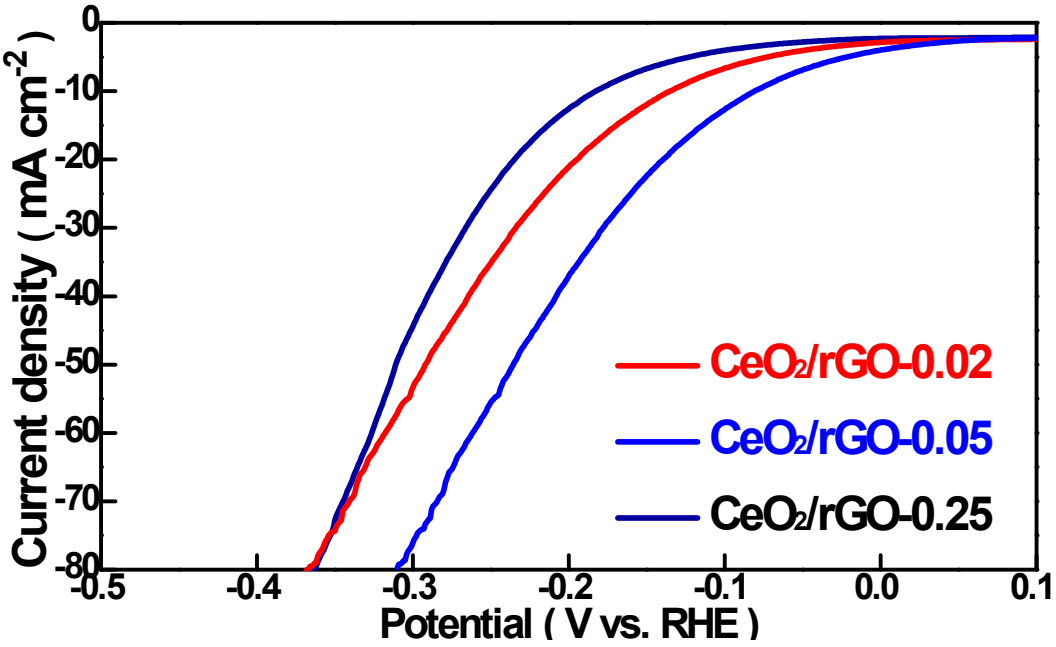

Figure S8. LSV curves of CeO_2/rGO NCPs with different addition of rGO.

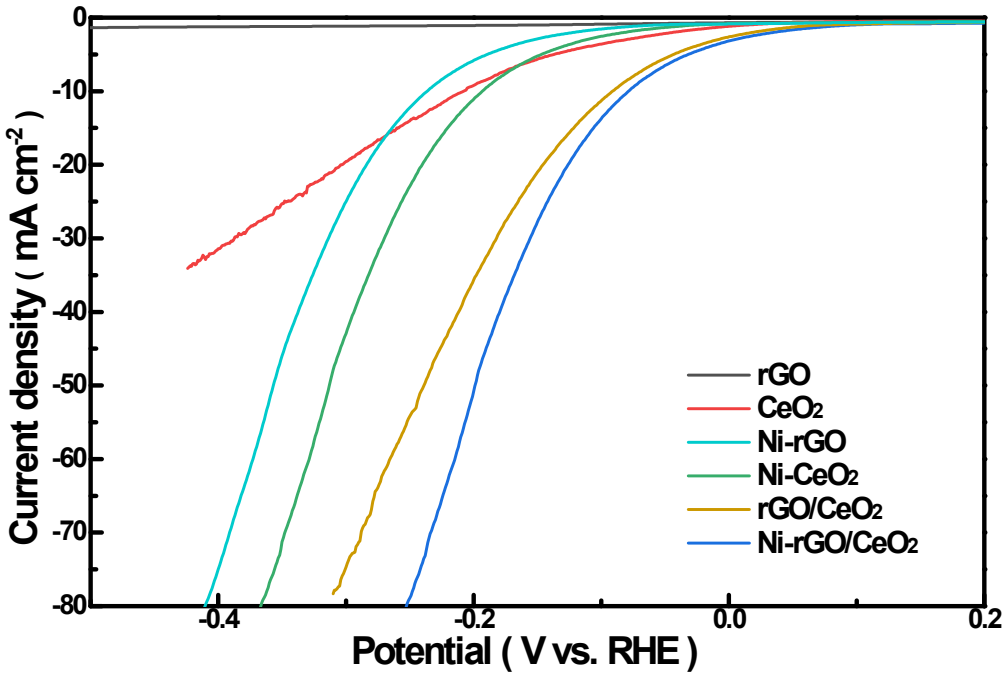

Figure S9. LSV curves of all the electrodes related to this study.

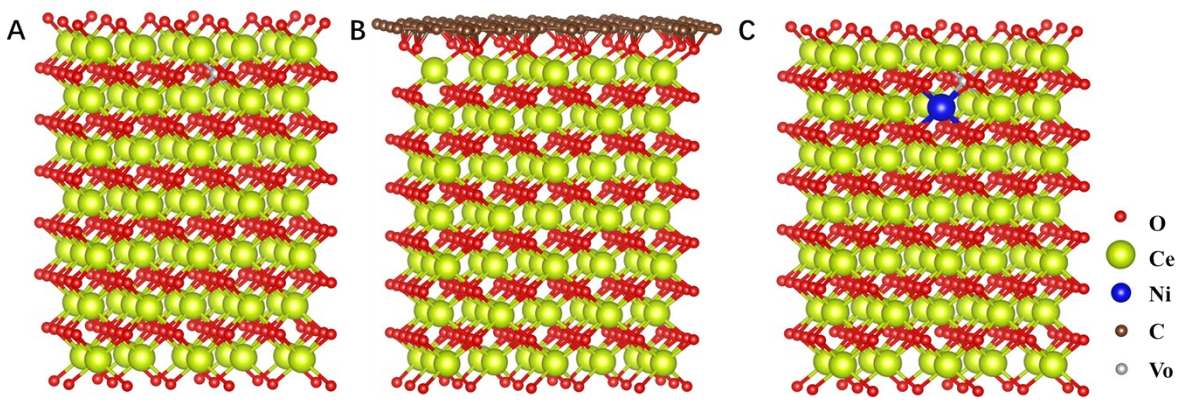

Figure S10. The structure models of (A) pristine CeO_2 after the removal of one O at the top surface layer, (B) CeO_2/rGO constructed by combining the graphene layer with the oxygen end from the CeO_2, and (C) Ni-CeO_2 with a V_O.

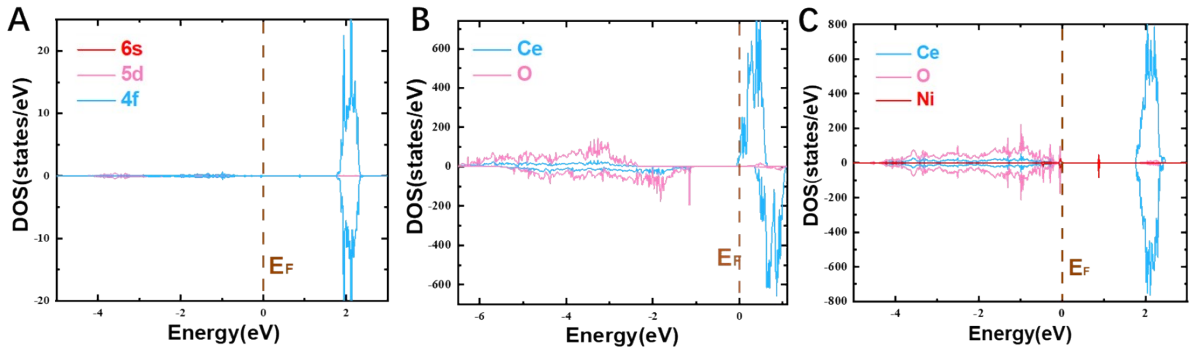

Figure S11. The PDOS of (A) CeO_2, (B) CeO_2 with V_O, and (C) Ni-CeO_2.

Table S1. Comparison of HER catalytic activity in alkaline solutions with high-performance catalyst materials reported in the literature

Catalytic materials	Electrolyte	Overpotential(mV)	Current density (mA cm^{-2})	References
Ni-rGO/CeO_2	**1M KOH**	**113**	**10**	**This work**
rGO-MoS_2	1M KOH	146	10	[2]
o-Ni_9S_8	1M NaOH	163	10	[3]
RGO/MoS_2/Pd	1M KOH	86	10	[4]
2D Mo-ReS_2	1M KOH	81	10	[5]
Ni_2P-Co_2P	1M KOH	94	10	[6]
$ReSe_2$	1M KOH	109	10	[7]
Cu-Mo-O	1M KOH	112	10	[8]
NiCoP/NF	1M KOH	80	10	[9]
N&S doped CNT	0.5M H_2SO_4	131	10	[10]

References

1 X. Hao, A. Yoko, C. Chen, K. Inoue, M. Saito, G. Seong, S. Takami, T. Adschiri, Y. Ikuhara, Atomic scale valence state distribution inside ultrafine CeO_2 nanocubes and its size dependence, *Small*, 2018, **14**, 1802915.

2 Y. Zhang, H. Zhou, H. Wang, Y. Zhang, D. D. Dionysiou, Synergistic effect of reduced graphene oxide and near-infrared light on MoS_2-mediated electrocatalytic hydrogen evolution, *Chem. Eng. J.*, 2021, **418**, 129343.

3 M. G. da Silva, C. M. Leite, M. A. Cordeiro, V. R. Mastelaro, E. R. Leite, One-Step Synthesis of Nickel Sulfides and Their Electrocatalytic Activities for Hydrogen Evolution Reaction: A Case Study of Crystalline h-NiS and o-Ni_9S_8 Nanoparticles, *ACS Appl. Energy Mater.*, 2020, **3**, 9498.

4 A. Pandey, A. Mukherjee, S. Chakrabarty, D. Chanda, S. Basu, Interface engineering of an RGO/MoS_2/Pd 2D heterostructure for electrocatalytic overall water splitting in alkaline medium, *ACS Appl. Mater. Interfaces*, 2019, **11**, 42094.

5 J. Xu, C. Fang, Z. Zhu, J. Wang, B. Yu, J. Zhang, Nanoscale engineering and Mo-doping of 2D ultrathin ReS_2 nanosheets for remarkable electrocatalytic hydrogen generation, *Nanoscale*, 2020, **12**, 17045.

6 Q. Cao, S. Hao, Y. Wu, K. Pei, W. You, R. Che, Interfacial charge redistribution in interconnected network of Ni2P–Co_2P boosting electrocatalytic hydrogen evolution in both acidic and alkaline conditions, *Chem. Eng. J.*, 2021, 130444.

7 I. S. Kwon, I. H. Kwak, S. Ju, S. Kang, S. Han, Y. C. Park, J. Park, J. Park, Adatom Doping of Transition Metals in $ReSe_2$ Nanosheets for Enhanced Electrocatalytic Hydrogen Evolution Reaction, *ACS Nano*, 2020, **14**, 12184.

8 A. Wang, L. Zhao, H. Liu, Z. Zhou, C. Li, Y. Xiang, W. Zhou, F. Hao, Dynamically controlled growth of Cu–Mo–O nanosheets for efficient electrocatalytic hydrogen evolution, *Journal of Materials Chemistry C*, 2020, **8**, 9337.

9 H. Liu, X. Ma, H. Hu, Y. Pan, W. Zhao, J. Liu, X. Zhao, J. Wang, Z. Yang, Q. Zhao, Robust NiCoP/CoP heterostructures for highly efficient hydrogen evolution electrocatalysis in alkaline solution, *ACS Appl. Mater. Interfaces*, 2019, **11**, 15528.

10 H. Wu, Z. Chen, F. Xiao, Y. Wang, E. Cao, S. Chen, S. Du, Y. Wu, Z. Ren, Tunable doping of N and S in carbon nanotubes by retarding pyrolysis-gas diffusion to promote electrocatalytic hydrogen evolution, *Chem. Comm.*, 2019, **55**, 10011.